

Optical tweezers with 2.5 kHz bandwidth video detection for single-colloid electrophoresis

Oliver Otto,¹ Christof Gutsche,¹ Friedrich Kremer,¹ and Ulrich F. Keyser^{1,2,a)}

¹*Institute of Experimental Physics I, Leipzig University, Linnéstr. 5, 04103 Leipzig, Germany*

²*Cavendish Laboratory, University of Cambridge, Madingley Road, Cambridge CB3 0HE, United Kingdom*

(Received 20 November 2007; accepted 29 January 2008; published online 28 February 2008)

We developed an optical tweezers setup to study the electrophoretic motion of colloids in an external electric field. The setup is based on standard components for illumination and video detection. Our video based optical tracking of the colloid motion has a time resolution of 0.2 ms, resulting in a bandwidth of 2.5 kHz. This enables calibration of the optical tweezers by Brownian motion without applying a quadrant photodetector. We demonstrate that our system has a spatial resolution of 0.5 nm and a force sensitivity of 20 fN using a Fourier algorithm to detect periodic oscillations of the trapped colloid caused by an external ac field. The electrophoretic mobility and zeta potential of a single colloid can be extracted in aqueous solution avoiding screening effects common for usual bulk measurements. © 2008 American Institute of Physics.

[DOI: 10.1063/1.2884147]

INTRODUCTION

Properties of colloidal dispersions have been studied intensively for decades. A fundamental understanding is of great importance in many fields of work, e.g., to analyze complex transport mechanisms in living organisms or to examine rheological phenomena of condensed matter. Colloidal dispersions find wide spread industrial applications as coatings, aerosols, ceramics, and drugs. Crucial for their properties are the size and charge of the colloids, both can be varied over a broad range, and thus the intercolloidal interactions can be adjusted. This makes colloidal dispersions an excellent model system to investigate fundamental issues in condensed matter physics.

The surface charge determines the colloids characteristics. However, it is not directly accessible in experiments. Investigations of electrorheological phenomena are based on two other quantities, the electrophoretic mobility μ and the associated zeta potential ζ .^{1,2}

Several methods are available for studying the mobility of colloidal dispersions. *Microscopic visual microelectrophoresis*² was a widespread technique until the 1980s and is based on the direct observation of individual particles moving in a dc electric field. Due to the Tyndall effect it is not the particle that is seen, but a bright dot on a dark background.² The difficulties in determining the position and direction of the colloids strongly limit the accuracy of this visual method.

Another one is *dynamic light scattering*, which is today available in commercial “Zetasizers” (Malvern, Herrenberg, Germany). In this measurement technique moving particles are illuminated by intersecting laser beams.³ As the frequency shift of the scattered light is proportional to the particle velocity, the average electrophoretic mobility of the

bulk solution can be calculated from the velocity distribution function.

A noninvasive way to investigate microscopic objects in a fluidic suspension are *optical tweezers*.⁴ Taking advantage of their properties, optical tweezers are ideal tools to carry out experiments with micrometer-sized objects in materials research, biological sciences, and soft matter physics.⁵⁻⁷ The idea behind optical tweezers is the application of a strongly focused laser beam to trap a small dielectric particle, allowing its manipulation in three dimensions. Their unique ability to hold and study single particles in a suitable medium without mechanical contact enables exciting new experiments in microrheology.^{8,9} For instance, optical tweezers allow detailed examinations of the electrophoretic mobility of colloids within nanometer accuracy. In comparison to the well-established Zetasizer measurements this technique gives insights to single particles effects that are not screened by many body interactions of a bulk solution.

The first part of this paper describes the optical tweezer setup including our self-assembled fluidic cell and the peripheral electronic devices. The movement of the bead is observed with video position detection. As we will show, the use of standard equipment is sufficient to perform position tracking of our colloids at 2.5 kHz bandwidth. At the current status of our experiments, we are able to measure with a temporal resolution of 0.2 ms and to determine the position of the colloid within a standard deviation of $\sigma < 0.5$ nm.

In the second part we discuss the drag force method and calibration via analyzing the power spectrum of the Brownian motion in the trap. The latter one requires a high bandwidth to obtain the typical Lorentzian shape^{10,11} and to provide reliable results. We verify that high-speed video position detection of the colloid is suitable for power spectra analysis. In contrast to quadrant photodiode based detection systems no voltage-to-meter conversion is necessary.

In the last part we show results from single-colloid-

^{a)}Electronic mail: keyser@physik.uni-leipzig.de.

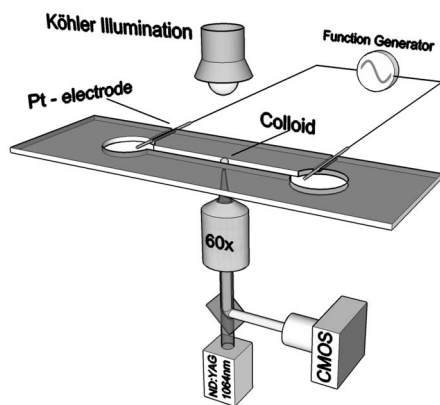


FIG. 1. (Color online) Sketch of fluidic cell and optical tweezer setup (not to scale), the dimensions of the PMMA cell: outer boundaries $76 \times 26 \times 1 \text{ mm}^3$, channel length: 30 mm, channel width: $300 \mu\text{m}$. The glass slides covering top and bottom are not shown.

electrophoresis experiments observing a $2.23 \mu\text{m}$ polystyrene bead in an environment of fixed ionic strength. After we apply an alternating electric field of known strength and frequency, we can capture the oscillations of the colloid. Due to the high spatial resolution of our video detection system, we are able to determine the position of the trapped bead within subnanometer precision. From this we derive the electrophoretic characteristics as the mobility μ and the ζ -potential of the colloid.

THE OPTICAL TWEEZERS SETUP

The optical tweezer setup (Fig. 1) is built around an inverted microscope (Axiovert 200, Carl Zeiss, Jena, Germany), which is designed for epillumination fluorescence microscopy. The optical trap is formed by a tightly focused diode pumped neodymium doped yttrium aluminum garnet laser beam (1064 nm 1 W, LCS-DTL 322, Laser 2000, Wessling, Germany), which is directed to the microscopy by the base port. At the chosen wavelength absorption and heating is reduced to a small magnitude, which is important as most of our experiments are carried out in water-based solvents.¹²

We use a closed-loop system [photodiode, personal computer (PC) with NI-PCI 6120 DAQ, National Instruments, München, Germany] to monitor and control the power of the laser before the beam is coupled into the microscope. A quarter-wave plate is employed to generate circular polarized light excluding effects due to reflection differences between the p - and s -part of the laser light. The beam is expanded, coupled into the back aperture of the water-immersion microscope objective (Olympus UPlanApo/IR, 60 \times , 1.20 W), and strongly focused to the trap center within the sample cell (Fig. 1).

Our sample cell is mounted on a XYZ piezostage (P-562.3, Physik Instrumente, Karlsruhe, Germany), which allows multi-axis motion with nanometer resolution. The position is controlled using a multichannel digital piezocontroller (E-710.3, Physik Instrumente, Karlsruhe, Germany) connected to a PC via the general purpose interface bus (GPIB) interface.

All measurements are carried out in a self-assembled fluidic cell that consists of a microscope slide at the top (thickness $d=1 \text{ mm}$) and a cover slip at the bottom ($d \approx 150 \mu\text{m}$) separated by a micromachined Poly(methyl methacrylate) (PMMA) spacer ($d=1 \text{ mm}$). We use UV-sensitive glue to adhere all three parts. The inner shape of the PMMA spacer defines the fluidic geometry for our experiments (Fig. 1). The main channel has a rectangular shape and is 30 mm long and $300 \mu\text{m}$ wide. Due to this design we obtain a linear electric field distribution, which results in a constant electric force within the channel. This was verified by finite-element calculations and experiments using the optical trap (not shown). The small-sized cross section of the channel leads to a high resistance, which exceeds all other resistors in the system (e.g., potential drop at double layer of electrodes) by at least a factor of 20. This guarantees that almost 100% of the applied electrical potential drops along the channel. Two holes drilled in the upper microscope slide connect the cell to a silicon/poly(tetrafluoroethylene) (PTFE) tubing system flushing electrolytes and colloids into the PMMA channel. The flow is controlled by a custom-built syringe pump. As we want to perform single-colloid electrophoresis, we continue flushing the cell after a bead was trapped to ensure that no other colloids are left in the cell. Two cylindrical Pt wires ($d=0.2 \text{ mm}$) connected to a function generator are embedded in the PMMA keyways serving as electrodes to apply an electric field (Fig. 1). A property of Pt electrodes is that gas bubbling due to electrochemical reactions is suppressed.^{13,14} This is important in order to realize long-term measurements without disturbance and to acquire reliable data.

The electric field is generated by a GPIB controlled function generator (HP33120A, Hewlett Packard, Böblingen, Germany) and amplified by a factor of 12.6 employing a custom-built electronic device. As the HP33120A allows measurements with different waveforms in a wide frequency range ($100 \mu\text{Hz}$ –15 MHz) and at amplitudes varying from $50 \text{ mV}_{\text{p.p.}}$ to $10 \text{ V}_{\text{p.p.}}$ (volt peak to peak), it is an optimal signal source for our electrophoretic experiments. The ac signal is recorded with an analog to digital converter card (NI-PCI 6120 DAQ, National Instruments, München, Germany) using an equal bandwidth as our video detection system.

The movement of the bead in the optical trap is observed via high-speed video position detection.^{15–17} For illuminating our sample cell we use a standard 150 W cold-light source (LQ 1700, Linos, Göttingen, Germany). At the current status of our experiments, we are able to perform online position tracking of our colloids with a temporal resolution of 0.2 ms. Two reasons enable us to measure with such a high temporal resolution: First, the video system is based on a complementary metal oxide semiconductor (CMOS) image sensor (MC1310 monochrome CMOS camera, Unterschleissheim, Germany and high performance camera link NI PCIe-1429, National Instruments, München, Germany), which is mounted to the left side port of our microscope. Compared to charge coupled device techniques CMOS allows high-speed image capture at a convenient signal-to-noise ratio.

At full resolution of 1280×1024 pixel our camera has a

specification of 500 frames/s. With a reduced region of interest (RoI), frame rates of more than 10,000 frames/s are possible. Due to the finite size of our colloids ($2\ \mu\text{m}$ at a system magnification of $0.2\ \mu\text{m}/\text{pixel}$), we are able to limit the RoI to 100×100 pixel. This increases our frame rate to 5000 frames/s, which is sufficient for almost all feasible measurements.

The second reason for obtaining high-speed video position detection is the online analysis using a cross-correlation based centroid-finding algorithm.^{18–20} As the huge amount of video data is not stored in the computer, this eliminates the resource-limiting bottleneck between the CPU, the random accessible memory, and the hard disk.

TRAP CALIBRATION—STIFFNESS DETERMINATION

Before force measurements can be done, the optical trap needs to be calibrated. In this paper we focus on the drag force method and calibration via analyzing the power spectrum of the Brownian motion of a bead in the trap.^{10,11} The drag force method is based on Stokes law,

$$F = 6\pi\eta rv, \quad (1)$$

where F is the viscous force, η is the viscosity of the medium, r the radius of the bead, and v its velocity relative to the surrounding solution. When the stage is moved a trapped colloid will experience a Stokes force and be displaced from its equilibrium position. This leads to a counteracting linear force (according to Hooke's law) arising from the harmonic potential at the center of the trap,

$$F = -k_{\text{trap}}x, \quad (2)$$

where F is the force, k_{trap} is the force constant, and x the measured amplitude of the displacement. By balancing both equations the trap stiffness can be calculated easily. In practice, we move the optical trap to $50\ \mu\text{m}$ above the cell surface and use the piezostage to exert a force on the bead and measure the distance from the trap center. Using Eq. (1) we compute the force with the bead radius and the viscosity of the electrolyte for several velocities and deduce the trap stiffness with Eq. (2).

We measured the trapping strength for different laser powers, obtaining a linear dependency (Fig. 2). In order to improve the reliability of our results the whole procedure is repeated several times. Statistics show that we are able to calibrate our optical tweezers within an accuracy of $\pm 5\%$.

As the drag force measurements are relatively slow and therefore just need a small bandwidth, video based position detection systems were limited to this calibration method. Due to the high temporal resolution of $0.2\ \text{ms}$ of our setup, we can verify the drag force calibration by analyzing the Brownian motion of the trapped bead. Originally this method was only accessible for imaging position detection systems using a quadrant photodiode (QPD).^{4,16,17} The thermal fluctuations $S(f)$ of a colloid in an optical trap can be described by a Lorentzian profile given by¹¹

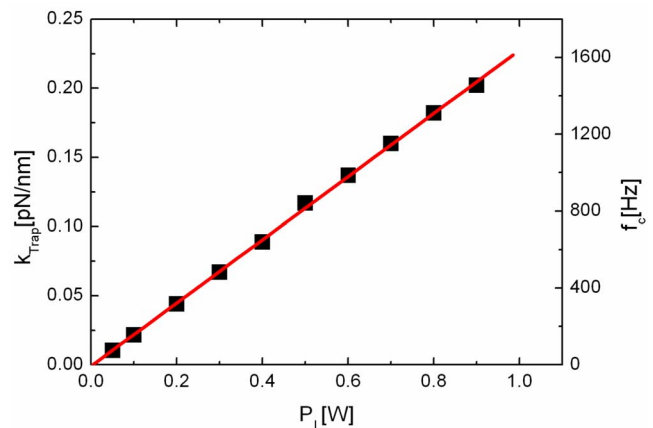


FIG. 2. (Color online) Trap stiffness (k_{trap}) and corner frequency (f_c) as a function of the laser power. Calibration was performed by the drag force method with a polystyrene (PS) colloid of $d=2.23\ \mu\text{m}$ in de-ionized water. The maximum error is indicated by the symbol size. The line shows a linear fit through our data.

$$S(f) = \frac{k_B T}{\gamma \pi^2 (f_c^2 + f^2)}, \quad (3)$$

where k_B is the Boltzmann constant, T is the temperature, and γ is the drag coefficient for a sphere with radius r moving in a viscous medium with viscosity η ,

$$\gamma = 6\pi\eta r, \quad (4)$$

and f_c is the characteristic frequency,

$$f_c = \frac{k_{\text{trap}}}{2\pi\gamma}. \quad (5)$$

The characteristic frequency f_c separates the bead fluctuation spectrum in two parts. For $f \ll f_c$ the bead feels the confinement of the trap and the power spectral density (PSD) is constant, whereas at higher frequencies the power spectrum decays as $1/f^2$, which is characteristic for free diffusion. The bead moves freely for short times.¹¹ In Fig. 3 we show for different laser powers P_L that our high-speed video detection system enables us to measure power spectra with high accuracy. The characteristic frequency is determined from an arctan least-squares fit after numerically integrating the Lorentzian profile. This procedure offers superior accuracy than fitting the PSD directly. From the characteristic frequency we calculate the trap stiffness using Eq. (5).

An advantage of the video based fluctuation analysis is the simplified calibration. When applying a QPD the power spectral density is obtained from the voltage output proportional to the bead position. As the displacement cannot be measured directly a secondary calibration is necessary. This calibration factor, the detector sensitivity, depends on several quantities, e.g., the signal amplification and the laser intensity.^{10,21} In our high-speed video detection system this factor is not important as the well-known system magnification enables us to measure the bead position directly in nanometers.

Comparison of both calibration methods, the drag force measurements and analyzing of the Brownian motion of a trapped bead, yields equal results. The characteristic frequen-

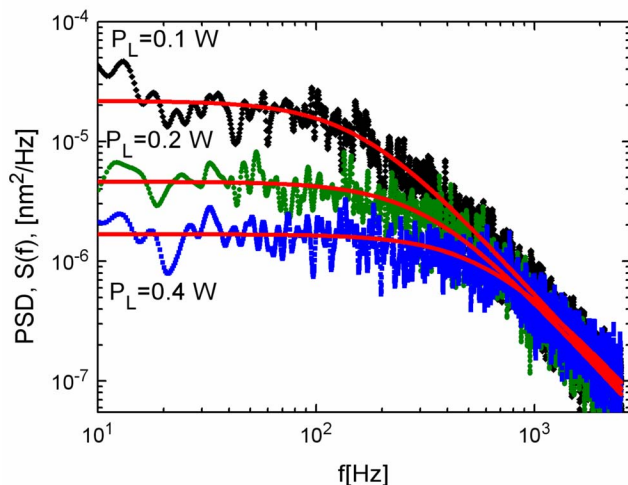


FIG. 3. (Color online) Power spectral density (PSD) of the Brownian motion of a PS colloid ($d=2.23 \mu\text{m}$, de-ionized water) as a function of frequency. We use the power spectra analysis to verify the drag force calibration for different laser powers [$P_L=0.1 \text{ W}$ ($f_c=157 \text{ Hz}$), $P_L=0.2 \text{ W}$ ($f_c=327 \text{ Hz}$), $P_L=0.4 \text{ W}$ ($f_c=621 \text{ Hz}$)].

cies f_c shown in Fig. 3 for laser powers $P_L=0.1 \text{ W}$, $P_L=0.2 \text{ W}$, and $P_L=0.4 \text{ W}$ fit well with the ones calculated from the trap stiffness k_{trap} in Fig. 2. In fact, the discrepancy is less than 5%, revealing the potential of our video detection system.

MEASUREMENTS

Once the trap stiffness is determined we are able to perform electrophoretic measurements.^{2,9,10,16,17} All experiments are carried out in the above-described fluidic cell with electrolytes of fixed ionic strength, valence, and pH value. After a colloid is trapped in the middle of the channel, the nanopositioning stage moves the optical trap to a level of $50 \mu\text{m}$ above the lower cover slip. The applied potential on the two Pt electrodes excites an electric field, which induces oscillating displacements of the bead. At electric field strengths of $E=63 \text{ V/cm}$ the sinusoidal response can be seen visually (Fig. 4).

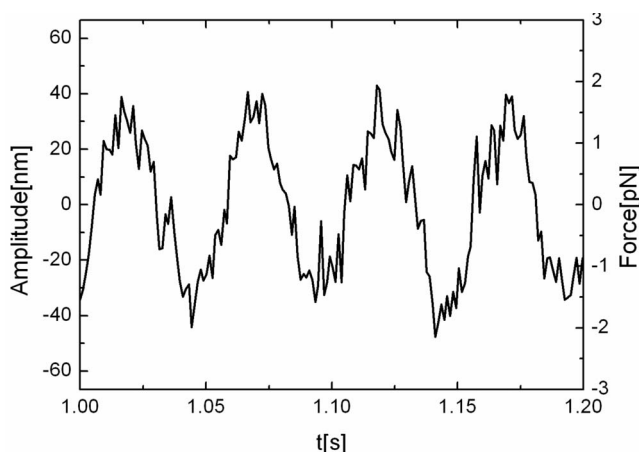


FIG. 4. Amplitude and force as a function of time of a $2.23 \mu\text{m}$ PS colloid moving in an ac field of $E=63 \text{ V/cm}$ at $f=20 \text{ Hz}$ in de-ionized water.

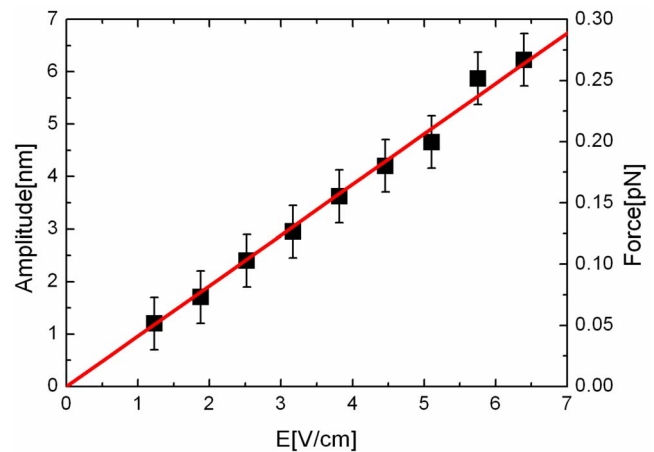


FIG. 5. (Color online) Amplitude and force as a function of the electric field of a negatively charged $2.23 \mu\text{m}$ PS colloid in $10^{-3} \text{ M KCL} + 10^{-4} \text{ M Tris}$ at a frequency of $f=80 \text{ Hz}$. We calculate the electrophoretic mobility $\mu = -(2.34 \pm 0.2) \times 10^{-8} \text{ m}^2/\text{V s}$ from the slope of the linear fit (closed line) of our experimental data [Eq. (9)]. The ζ -potential is obtained from the Helmholtz-Smoluchowski equation to $\zeta \approx -33 \text{ mV}$.

In long-term measurements these parameters lead to electrochemical reactions as the electrolysis of water. Therefore we perform our experiments at much smaller field strengths ($E < 8 \text{ V/cm}$) without losing resolution. The increase in electrochemical stability leads to a decrease in the amplitude of the oscillating bead, which gives rise to a different analysis method, as simple fit routines do not provide reliable results. A very powerful tool to extract information from a noisy signal is the Fourier algorithm. To ensure complete control on our data, we implemented a Fourier transform algorithm by ourselves using C++. The source code was compiled in a dynamic link library interfacing our LABVIEW data acquisition tool.

The mathematical properties of Fourier transformation can be exploited to increase the signal-to-noise ratio dramatically as it averages the number of samples in the resulting spectrum. This, in conjunction with the fact that we know the frequency of the externally applied electric fields, yields in a spatial resolution of 0.5 nm or 20 fN ($k_{\text{trap}}=0.042 \text{ pN/nm}$, $f=80 \text{ Hz}$).

Figure 5 summarizes measurements on a single $2.23 \mu\text{m}$ polystyrene (PS) colloid stabilized by sulfate groups (Micro-particles, Berlin, Germany).²² The amplitude and force of the oscillating bead were captured at electric field strengths between 0.5 and 8 V/cm . The whole experiment was performed in $10^{-3} \text{ M KCL} + 10^{-4} \text{ M Tris}$ solution. Trishydroxymethylaminomethane (Tris) is a buffer used to stabilize the electrolyte at a pH value of 7. At the end of each sequence we repeated the measurement at $E=4.1 \text{ V/cm}$ to exclude hysteresis effects. The graph shown in Fig. 5 highlights the typical linear dependency of amplitude and force of the oscillating bead on the electric field. Generally the correlation coefficient was >0.99 . As we explain below, we can use the gradient of the experimental data to derive important electrophoretic characteristics of the colloid.

The electrophoretic mobility μ as one quantity of interest is associated with the magnitude of the drift velocity v_{drift} and the electric field E by²

$$\mu = \frac{v_{\text{drift}}}{E}. \quad (6)$$

The effective velocity v_{eff} of the colloid consists of a Stokes term (1) and drift term (6),

$$v_{\text{eff}} = \frac{F}{6\pi\eta r} + \mu E. \quad (7)$$

For the sake of simplicity no vectorial representation of the quantities is given. Using the fact that the colloid oscillates at a frequency f with an amplitude a , the average value v_{eff} of one period is given by

$$v_{\text{eff}} = 4af. \quad (8)$$

Substituting F from Eq. (2) leads to a relation between the electrophoretic mobility μ , the electric field E , and the amplitude of the colloidal oscillations a ,

$$|\mu| = \left(4f + \frac{k_{\text{trap}}}{6\pi\eta r}\right)m, \quad (9)$$

where $m = a/E$ is the slope of the linear fit of Fig. 5.

The electrophoretic mobility is related to the ζ -potential by the well-known Helmholtz–Smoluchowski equation,¹

$$\mu = \frac{\varepsilon_r \varepsilon_0}{\eta} \zeta, \quad (10)$$

where ε_r is the relative permittivity and ε_0 is the permittivity of free space.²³ Smoluchowski's theory is valid for particles with curvature radius exceeding the Debye length κ^{-1} ,²

$$\kappa a \gg 1, \quad (11)$$

where κ is defined as

$$\kappa = \sqrt{\frac{\sum e^2 Z_i^2 n_i}{\varepsilon_r \varepsilon_0 k_B T}}, \quad (12)$$

with e the elementary charge, Z_i the charge number, and n_i the number concentration of each ionic species in the solvent.

For our experiments we used a negatively charged 2.23 μm PS colloid oscillating in 10^{-3}M KCL electrolyte solution buffered with 10^{-4}M Tris at an external frequency of $f = 80$ Hz. The polarity of the colloid determines the negative sign of the mobility and the ζ -potential. From the data shown in Fig. 5 and Eqs. (9) and (10) we can calculate the electrophoretic mobility to $\mu = -(2.34 \pm 0.2) \times 10^{-8} \text{ m}^2/\text{V s}$ and the ζ -potential to $\zeta \approx -33$ mV. As the whole system is very sensitive even to minor impurities, several control measurements were carried out showing results within the experimental error. Gutsche *et al.* measured the pair interaction potential between a single pair of colloids applying the Derjaguin-Landau-Verwey-Overbeek theory.⁸ Using a formula derived by Crocker and Grier⁶ they obtain a ζ -potential of $\zeta \approx -31$ mV (surface charge of approximately 220.000). This value is in good agreement with our data with a deviation less than 8%.

DISCUSSION

An alternative to video position detection is to image the motion of a trapped bead directly onto a quadrant

photodiode.¹⁰ This technique reaches bandwidths exceeding 100 kHz and a spatial resolution up to 0.1 nm. However, because of the ease of use and the straightforward calibration video position detection has been widely adopted, but was typically limited by 5 nm resolution and a frame rate of 60 Hz.¹⁶ Recently different approaches were developed increasing the performance. Biancaniello and Crocker¹⁶ described an optical tweezer setup based on laser illumination and a CMOS position detector. Due to the high frame rate all images are firstly buffered in the random access memory of the camera and transferred to the computer after the measurement. This procedure allows studying the motion of particles offline within an accuracy of 1 nm and 10 kHz bandwidth, but demand great experimental skill to overcome technical problems, e.g., interferences due to coherent laser illumination.

Keen *et al.*¹⁷ compared high-speed cameras and QPD to measure displacements in optical tweezers. Using standard equipment they achieve 2 kHz bandwidth and a spatial resolution of 5 nm for video detection.

In our experiments we consequently overcome the described problems and speed limiting bottlenecks of high-speed video detection. Although we just use standard Köhler illumination with a cold-light source, we are able to measure with 2.5 kHz bandwidth avoiding coherence effects (interference and speckle) of laser illumination. The high performance camera link interface in combination with our self-implemented Fourier position-tracking algorithm enables us to locate a trapped bead with a spatial resolution down to 0.5 nm (at fixed external frequency), which is a decade better as reported elsewhere for video position tracking.^{4,17} The high performance of our optical tweezers setup gives rise to a variety of experiments, e.g., measuring the mobility of single colloids in various media or studies of DNA-protein interactions with a force clamp based on video detection.

CONCLUSION

In the present work we introduced an optical tweezer setup for studying the motion of charged colloids with subnanometer resolution. Using only standard components for illumination and video detection, we achieve a temporal resolution of 0.2 ms. This high-speed position tracking allows calibration of the optical trap by power spectrum analysis of the Brownian motion of the colloid. The results are in excellent agreement with calibration based on Stokes drag force. With the calibrated trap we are able to detect electrophoretic movements in an periodic electrical field down to 0.5 nm which results in a force resolution of 20 fN implementing a Fourier algorithm. In future we plan to study single-colloid electrophoresis in environments of varying ionic strengths, pH value, and valence. We expect a deeper understanding of fundamental phenomena in colloid science, e.g., charge inversion²⁴ and the interaction of electric and hydrodynamic friction.²⁵

ACKNOWLEDGMENTS

The authors would like to thank Armand Ajdari for fruitful discussion and Ralf Seidel for his help with program-

ming. We acknowledge valuable conversations with Gunter Stober and Tilman Butz about Fourier transformation. This work was supported by the DFG and the Emmy Noether Program.

- ¹R. J. Hunter, *Zeta Potential in Colloid Science: Principles and Applications* (Academic, London, 1981).
- ²A. V. Delgado, F. Gonzalez-Caballero, R. J. Hunter, L. K. Koopal, and J. Lyklema, *J. Colloid Interface Sci.* **309**, 194 (2007).
- ³M. Minor, A. J. van der Linde, H. P. van Leeuwen, and J. Lyklema, *J. Colloid Interface Sci.* **189**, 370 (1997).
- ⁴K. C. Neuman and S. M. Block, *Rev. Sci. Instrum.* **75**, 2787 (2004).
- ⁵M. Salomo, K. Kegler, C. Gutsche, M. Struhalla, J. Reinmuth, W. Skokow, U. Hahn, and F. Kremer, *Colloid Polym. Sci.* **284**, 1325 (2006).
- ⁶J. C. Crocker and D. G. Grier, *Phys. Rev. Lett.* **77**, 1897 (1996).
- ⁷T. Sugimoto, T. Takahashi, H. Itoh, S. Sato, A. Muramatsu, *Langmuir* **13**, 5528 (1997).
- ⁸C. Gutsche, U. F. Keyser, K. Kegler, F. Kremer, P. Linse, *Phys. Rev. E* **76**, 031403 (2007).
- ⁹G. S. Roberts, T. A. Wood, W. J. Frith, P. Bartlett, *J. Chem. Phys.* **126**, 194503 (2007).
- ¹⁰R. Galneder, V. Kahl, A. Arbutova, M. Rebecchi, J. O. Rädler, and S. McLaughlin, *Biophys. J.* **80**, 2298 (2001).
- ¹¹F. Gittes, and C. F. Schmidt, *Methods Cell Biol.* **55**, 129 (1998).
- ¹²G. M. Hale and M. R. Querry, *Appl. Opt.* **12**, 555 (1973).
- ¹³E. E. Uzgiris, *Rev. Sci. Instrum.* **45**, 74 (1974).
- ¹⁴A. Norlin, J. Pan, and C. Leygraf, *Biomol. Eng.* **19**, 67 (2002).
- ¹⁵J. C. Crocker and D. G. Grier, *J. Colloid Interface Sci.* **179**, 298 (1996).
- ¹⁶P. L. Biancaneello and J. C. Crocker, *Rev. Sci. Instrum.* **77**, 113702 (2006).
- ¹⁷S. Keen, J. Leach, G. Gibson, and M. J. Padgett, *J. Opt. A, Pure Appl. Opt.* **9**, 264 (2007).
- ¹⁸M. K. Cheezum, W. F. Walker, and W. H. Guilford, *Biophys. J.* **81**, 2378 (2001).
- ¹⁹A. Yildiz, J. N. Forkey, S. A. McKinney, T. Ha, Y. E. Goldman, and P. R. Selvin, *Science* **300**, 2061 (2003).
- ²⁰J. Gelles, B. J. Schnapp, and M. P. Sheetz, *Nature (London)* **331**, 450 (1988).
- ²¹D. Selmeczi, S. F. Tolic-Norrelykke, E. Schaffer, P. H. Hagedorn, S. Mosler, K. Berg-Sorensen, N. B. Larsen, and H. Flyvbjerg, *Acta Phys. Pol. B* **38**, 2407 (2007).
- ²²N. Garbow, M. Evers, T. Palberg, and T. Okubo, *J. Phys.: Condens. Matter* **16**, 3835 (2004).
- ²³V. Lobaskin, B. Dünweg, and C. Holm, *J. Phys.: Condens. Matter* **16**, 4063 (2004).
- ²⁴K. Besteman, M. A. G. Zevenbergen, H. A. Heering, and S. G. Lemay, *Phys. Rev. Lett.* **93**, 170802 (2004).
- ²⁵Y. W. Kim and R. R. Netz, *J. Chem. Phys.* **124**, 114709 (2006).